IET Nanobiotechnology

Research Article

IET Journals
The Institution of Engineering and Technology

Green synthesis of gold nanoparticles using *Citrus maxima* peel extract and their catalytic/ antibacterial activities

ISSN 1751-8741
Received on 7th September 2016
Revised 17th November 2016
Accepted on 25th November 2016
E-First on 24th March 2017
doi: 10.1049/iet-nbt.2016.0183
www.ietdl.org

Chun-Gang Yuan[1] ✉, Can Huo[1], Bing Gui[1], Wei-Ping Cao[2]

[1]School of Environmental Science & Engineering, North China Electric Power University, Baoding 071000, People's Republic of China
[2]Institute of Plant Protection, Hebei Academy of Agricultural and Forestry Sciences, Baoding 071000, People's Republic of China
✉ *E-mail: chungangyuan@hotmail.com*

Abstract: The peel of *Citrus maxima* (*C. maxima*) is the primary byproducts during the process of fruit or juice in food industries, and it was always considered as biomass waste for further treatments. In this study, the authors reported a simple and eco-friendly method to synthesise gold nanoparticles (AuNPs) using *C. maxima* peel extract as reducing and capping agents. The synthesised AuNPs were characterised by UV–visible spectrum, X-ray diffraction (XRD), transmission electron microscope (TEM) and Fourier-transform infrared spectroscopy (FTIR). The UV–visible spectrum of the AuNPs colloid showed a characteristic peak at 540 nm. The peaks of XRD analysis at (2θ) 38.30°, 44.28°, 64.62°, 77.57° and 81.75° were assigned to (111), (200), (220), (311) and (222) planes of the face-centered cubic (fcc) lattice of gold. The TEM images showed that AuNPs were nearly spherical in shape with the size of 8–25 nm. The FTIR spectrum revealed that some bioactive compounds capped the surface of synthesised AuNPs. The biosynthesised AuNPs performed strong catalytic activity in degradation of 4-nitrophenol to 4-aminophenol and good antibacterial activity against both gram negative (*Escherichia coli*) and gram positive (*Staphylococcus aureus*) bacterium. The synthesis procedure was proved simple, cost effective and environment friendly.

1 Introduction

Gold nanoparticles (AuNPs) have been proved with strong antibacterial [1] and catalytic activities [2]. They have been applied in many fields and attracted more and more attentions in recent years [3–7]. Many synthesis methods including some green and eco-friendly methods for nanoparticles (NPs) have been developed [8–11]. The biosynthesis methods using microorganism or extract of plants as reducing and capping agents are considered as nontoxic, simple, low-cost and environment benign methods for the preparation of NPs [12–14]. Among these biosynthesis methods, phytobiosynthesis is regarded as the most promising route due to the fact that the natural available plants are usually inexpensive, and the process of synthesis is feasible for large-scale productions [13–15].

The researchers in India can be regarded as the pioneers in this new field. Shankar *et al.* [16] used geranium leaf extract to reduce gold ions and stabilise the AuNPs more than ten years ago. To the best of our knowledge, this should be the first study about the biosynthesis of AuNPs using plant extract. Later on, the authors found the leaf of neem could also be applied for the preparation of AuNPs [17], and the reaction was more rapid compared with the previous study. The morphology of AuNPs was predominantly in planar and spherical shapes. Flavanones and terpenoids, which are abundant in the neem leaf acted as the reducing, stabiliser and capping agents for NPs without aggregation. Lemongrass was also used to synthesise AuNPs [18]. The shapes of AuNPs could be adjusted by the different fractions of lemongrass extract. Until now, the strategy of phytosynthesis has been greatly developed. Many plants have already been applied to synthesise AuNPs, such as *Zingiber Officinale* [19], *Dioscore Bulbifera* [20] and *Barbated Skullcup* [21]. In addition to metallic NPs, some metal–oxide NPs were also synthesised by natural plant extracts [14, 22, 23].

Citrus maxima (*C. maxima*) is one of the members of *Rutaceae* family and universally distributed in the southeast of Asia, especially in the south of the Yangtze River in China. The peel of *C. maxima* is the primary byproducts during the process of fruit or juice in food industries [24], and it was always considered as biomass waste for further treatments. It has been proved that a variety of flavonoids including narirutin, naringin, hesperidin, eriocitrin and neohesperidin were present in the peels and pulps [25]. These kinds of compounds are also known to possess antiviral, anticancer, anti-inflammatory, antiallergenic and analgesic activities. Herein, the peel extract of *C. maxima* can potentially be used as reducing and capping agents for the preparation of AuNPs. Although the study about the biosynthesis of AuNPs using *citrus* flesh or pulps has been reported recently [26], there is no report to synthesise noble metal nanoparticles using *C. maxima* peels [27]. Compared with fruit flesh, *C. maxima* peels will be more cost effective. In addition, the growth of plants is usually influenced by regions and climates. How to logically obtain and economically store the biomass is another critical issue for the real applications and scaling-up of phytobiosynthesis methods. *C. maxima* peels can be easily obtained, dried and stored for a long time. These features of *C. maxima* peels enable the proposed method more feasible and practical. To synthesise AuNPs using *C. maxima* peel not only provides us a facile biosynthesis method but also be valuable for the beneficial utilisation of agriculture waste.

The catalytic property of AuNPs is used in many fields, especially in removing contaminants in wastewater. Many researchers have reported that AuNPs synthesised by plant extract were used as catalysts for the degradation of 4-nitrophenol (4-NP) [28] and methylene blue [29]. The biosynthesised AuNPs showed much better catalytic activity than chemically synthesised AuNPs [30] without adding any toxic or harmful substances for their preparations. AuNPs are also applied as antibacterial agents. Some reports revealed that AuNPs synthesised via plant extract could kill or inhibit both gram negative and gram positive bacteria [31].

In this study, a new, simple and green biosynthesis method of AuNPs using peel extract of *C. maxima* was successfully developed. The formation of AuNPs was monitored by UV–visible spectra. The size and morphology of the obtained AuNPs were characterised by high-resolution transmission electron microscopy (HRTEM) with X-ray energy dispersive detector (EDS). Their crystalline and the chemical groups capped on the surface of the particles were further characterised by powder X-ray diffraction (XRD) and Fourier-transform infrared spectroscopy (FTIR). The catalytic and antibacterial activities of the obtained AuNPs were also investigated via the experiments of 4-NP degradation and

inhibition tests against both *Escherichia coli* (*E. coli*) and *Staphylococcus aureus* (*S. auerus*).

2 Materials and methods

2.1 Materials

C. maxima was purchased from a local market in Baoding, China. Chloroauric acid ($HAuCl_4{\cdot}4H_2O$) was purchased from Sinopharm Chemical Reagent Co. Ltd. A stock solution of $HAuCl_4$ was prepared by dissolve 1.0 g $HAuCl_4{\cdot}4H_2O$ in 24.28 ml distilled water. All glasses were cleaned with aqua regia solution and thoroughly rinsed with distilled water and dried in oven before use.

2.2 Preparation of the extract of C. maxima peel

The peel of *C. maxima* was dried in an oven at 50°C and ground to pieces. The extract was prepared by taking 1.0 g of peel into 100 ml deionised water and boiled for 10 min. The working extract was obtained by filtration the original extract through a microporous membrane and stored in a refrigerator at 4°C for use.

2.3 Synthesis of AuNPs using the extract of C. maxima peel

To biosynthesise AuNPs, 100 µl of chloroauric acid (100 mM) was added into 10 ml of *C. maxima* extract and shaken at room temperature. The colour of the mixture changed from light yellow to purple indicating the formation of AuNPs in the solution. The reaction mixture was then centrifuged at 16,000 rpm for 10 min and the pellet was washed with distilled water for three times to remove any possible impurities on the surface of the NPs.

The effect of $HAuCl_4$ concentration was investigated by varying the volume of the $HAuCl_4$ working solution. 50, 100, 150 and 200 µl of $HAuCl_4$ (100 mM) were added into 10 ml of the peel extract, respectively. To study the effect of incubation temperature, the reaction mixtures containing 100 µl of $HAuCl_4$ (100 mM) aqueous solution and 10 ml of the peel extract were placed in water bath at 40, 50, 60 and 70°C, respectively. The effect of pH was studied by adjusting the pH values of *C. maxima* peel extract with 0.1 M HCl and 0.1 M NaOH solutions. The pH values were adjusted to 3.0, 5.0, 7.0, 9.0 and 11.0. 100 µl of $HAuCl_4$ aqueous solution were added to 10 ml of the above solution at different pH values. The formation of AuNPs was monitored by a UV–vis spectrometer. All of the experiments were carried out in triplicates.

2.4 Characterisation of the synthesised AuNPs

The formation of AuNPs was scanned by UV-vis spectra (Pgenenal, China) from 300 to 800 nm at a resolution of 1 nm. The sizes and shapes of the AuNPs were measured by transmission electron microscope (Tecnai G2 F20 S-TWIN, FEI/Netherland). Samples were prepared by placing a drop of solution sample onto a carbon-coated Cu grid and evaporated in ambient condition. The microscope was also equipped with a genesis liquid nitrogen cooled energy-dispersive X-ray analysis (EDX) detector for detailed elemental analysis. X-ray powder diffractometer (D8 ADVENCE, Bruker/Switzerland) with Cu-Kα radiation (λ = 1.5418 Å) with a scan speed of 2°/min was used to analyse the crystalline structure of AuNPs.

Fourier-transform infrared spectra (FTIR) were recorded using Magna-IR 750 (America) in order to analyse the functional groups in *C. maxima* peel which are possibly involved in the synthesis of AuNPs. FTIR spectrophotometer was operated in the spectral range of 4000–400 cm^{-1} with resolution of 4 cm^{-1}.

2.5 Catalytic activity of AuNPs

The degradation of 4-NP to 4-aminophenol (4-AP) by $NaBH_4$ was performed as a probe for the study of the catalytic activity of AuNPs [32]. In a standard quartz cell, 20 µl of 4-NP (20 mM) solution and 400 µl of fresh $NaBH_4$ (2.5 M) solution were mixed in 60 µl of the prepared AuNPs colloidal solution. The appropriate deionised water was added to keep its final volume constant (3 ml). The process of reaction was monitored by a UV–vis spectrometer. The different volumes of the AuNPs (20 and 40 µl) solution were added to measure the degradation rates.

2.6 Antibacterial activity of AuNPs

The extract of *C. maxima* peel, the biosynthesised AuNPs and gentamicin were used for the inhibition tests against both gram positive (*S. aureus*) and gram negative (*E. coli*) bacteria. The different concentrations of AuNPs were used to evaluate the antibacterial abilities. *S. aureus* and *E. coli* were cultured in nutrient broth at 37°C for 18 h. 100 µl of the bacterial suspensions were coated on the Luria-Bertani (LB) solid medium, respectively. 10 min later, five Oxford cups were placed on the above LB solid medium. 50 µl of *C. maxima* peel extract, AuNPs (1.0, 1.5 and 2.0 mM) and gentamicin were added into the Oxford cups, respectively. The Petri dishes were incubated in the incubator at 37°C for 24 h. After culture, the zones of inhibition were observed and measured. Three replicates were tested for each bacteria strain.

3 Results and discussion

3.1 Biosynthesis of AuNPs

AuNPs always appears in ruddiness colour in aqueous solution due to excitation of surface plasmon vibrations [21]. The formation of AuNPs was confirmed by the colour change from pale yellow to purple after incubation for about 1 h. The synthesised AuNPs were initially investigated by UV–vis spectroscopy. The intensity and width of the surface plasmon resonance (SPR) peaks depend on the size, morphology, spatial orientation, optical constants of the particles and the embedding medium as well [33, 34]. Here, the reaction conditions such as concentration, reaction temperature and pH were investigated and discussed.

3.1.1 Effect of chloroauric acid concentration: Fig. 1*a* shows the visual observation of AuNPs at various $HAuCl_4$ concentrations after 2 h reaction. It was evident that the colours of the four samples were different, which indicated that the sizes or morphologies of the synthesised AuNPs were different. When the lower concentration of $HAuCl_4$ was applied, the reduction rate was faster during the initial time span for the abundant presence of biomolecules in the mixture at the beginning of the reaction.

It was also confirmed by UV–vis spectrum in Fig. 1*b*(*A*). A characteristic absorption band at 540 nm was observed after 0.5 h reaction. With the reaction going on and more AuNPs being synthesised, the SPR band was lightly shifted from 540 to 554 nm when the elevated concentration of AuNPs was applied. The peak shift indicated that the sizes and shapes of the NPs were slightly changed compared with the initial colloid. The SPR bands were sharper and symmetric at the lower concentrations of $HAuCl_4$, which indicated that the biosynthesised AuNPs were monodispersed in the solution [35]. The SPR bands appeared 2 h or longer after the extract were mixed with the higher concentrations of Au^{3+} solution (Fig. 1*b*(*B*)–(*D*)). The prolonged appearance of AuNPs in solution was probably owing to the excessive Au^{3+} ions in the mixture. The abundant Au^{3+} ions were reduced to Au^0 and produced a large number of opportunities for nucleation, which would take longer time for Au^0 to grow into larger clusters [36]. After the mixture reacted for 24 h, the intensities of SPR bands at the higher concentrations of $HAuCl_4$ solution were much stronger than that at the lower concentrations. The quantity of AuNPs formed at the higher concentrations of $HAuCl_4$ was larger than that at the lower concentrations. An interesting phenomenon was observed that a weak absorption peak appeared at 680 nm. The peak lightly blue shifted and disappeared with the reaction. It might be due to the agglomeration of the formed AuNPs in solution or the particles in non-spherical shapes [37]. The peaks lightly blue shifted and disappeared when the heterogeneous AuNPs became homogeneous and monodispersive.

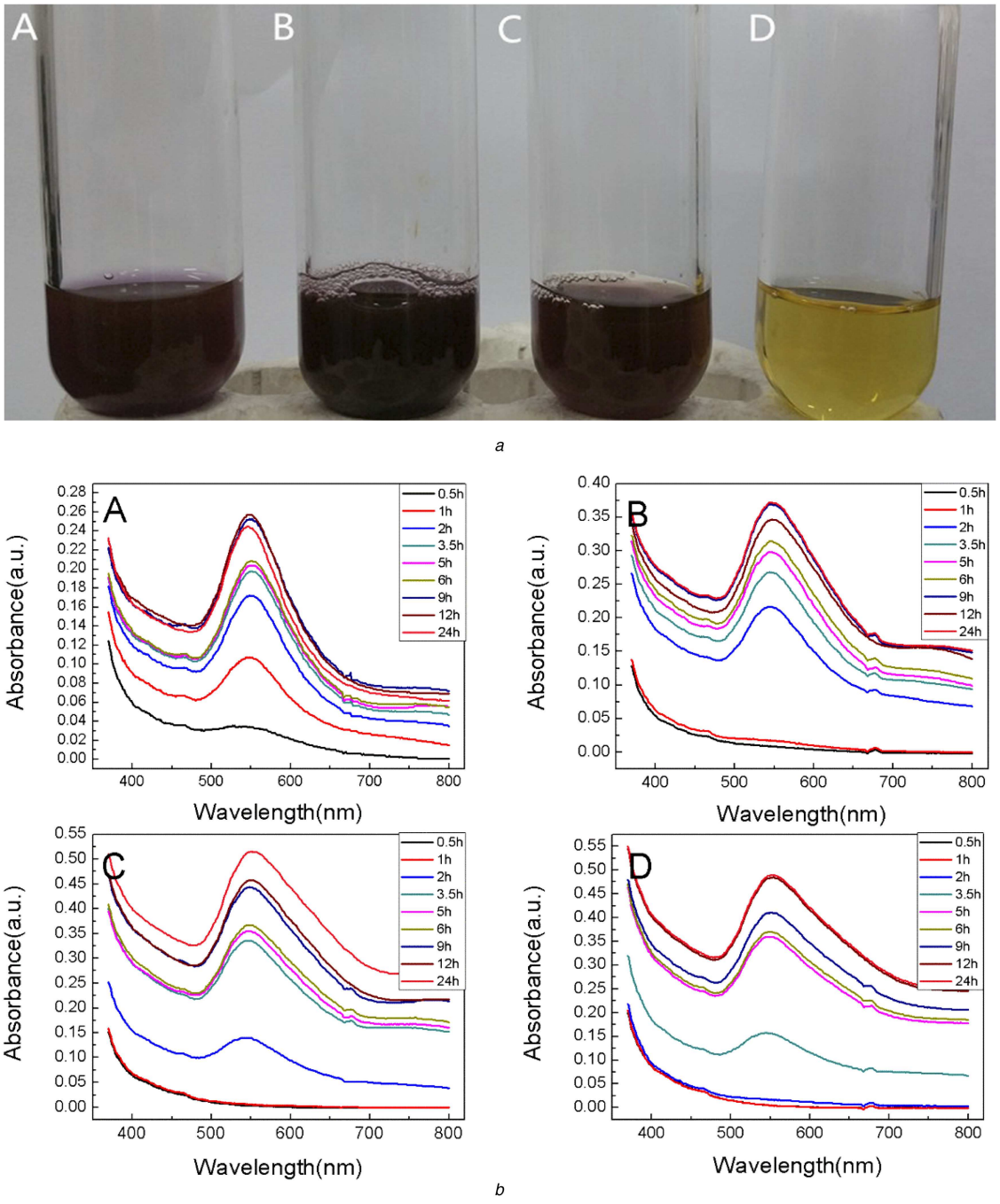

Fig. 1 *Effect of chloroauric acid concentration*

(a) Visual observation of reaction mixture after 2 h with different chloroauric acid concentrations (A) 0.5 mM, (B) 1 mM, (C) 1.5 mM, (D) 2 mM, ***(b)*** UV–vis absorption spectrum of AuNPs at various time intervals with different concentrations ((A) 0.5 mM, (B) 1 mM, (C) 1.5 mM, (D) 2 mM)

3.1.2 Effect of reaction temperature: Fig. 2*a* shows the UV–vis spectra of AuNPs at the different reaction temperatures. Temperature is one of the important parameters that influence the stability, activity and chemical characters of NPs [38]. In this study, a characteristic SPR band appeared after 5 min reaction when 70°C was employed.

The colour of the mixture was purple. There was no colour changing or absorption band in 5 min at 40, 50 and 60°C. With the reaction time going on, the SPR bands gradually appeared in all of the four samples. The intensities of the absorption peaks increased, which indicated more AuNPs were synthesised in the solution. In Fig. 2*a*(*D*), the maximum intensity of the peak appeared after 30 min reaction due to the exhaustive conversion of gold ions to AuNPs. Furthermore, the higher temperatures led to the higher reaction rates, which were confirmed by the UV–vis spectra shown in Fig. 2*b*. The intensity of the peak increased with the temperature increasing during the same incubation time. Fig. 2*a* and *b* also show that there was no significant influence of the temperature on the stability of AuNPs without any shifting and broadening of SPR band.

3.1.3 Effect of pH: pH plays a crucial role during the biosynthesis process of AuNPs. Fig. 3 shows the SPR bands of the AuNPs synthesised by the extract of *C. maxima* peel under various pH conditions (3.0, 5.0, 7.0, 9.0 and 11.0) at room temperature. An elevated pH value caused the intensity of the peaks increasing. The SPR band blue shifted gradually from 556 to 543 nm, which indicated that the AuNPs sizes decreased [39]. The conditions at higher pH could probably enhance the reaction rate and boost the homogeneous nucleation. On the contrary, the reaction rate was slow under the acidic conditions. It induced the heterogeneous nucleation and secondary nucleation of small AuNPs seeds [39], which gave rise to enlarge the sizes of AuNPs. Therefore, the sizes and shapes of AuNPs could be regulated by adjusting the pH of the reaction solution.

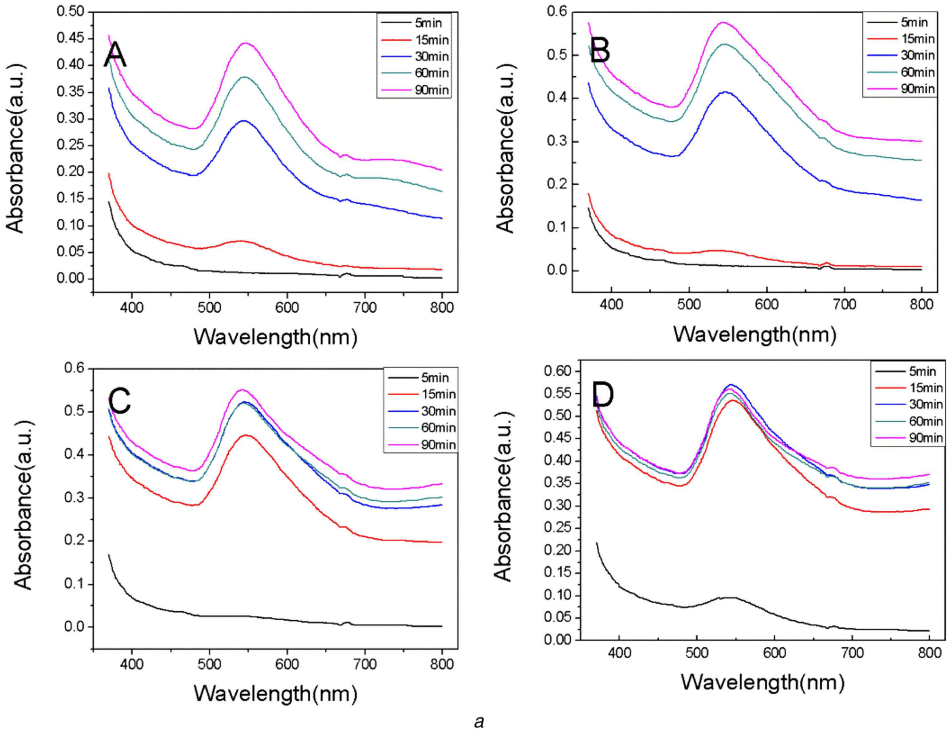

a

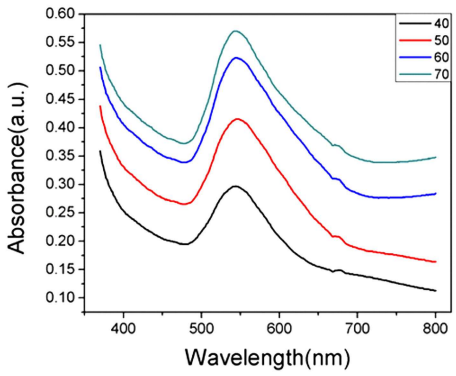

b

Fig. 2 *UV–vis spectra of AuNPs at different temperatures*
(a) UV–vis spectra of biosynthesised AuNPs at different temperatures (A) 40°C, (B) 50°C, (C) 60°C, (D) 70°C, ***(b)*** UV–vis spectra of AuNPs at different temperatures

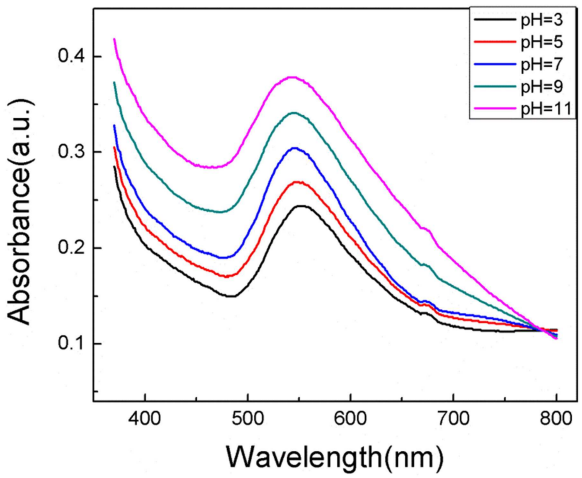

Fig. 3 *UV–vis spectra of AuNPs at different pH*

3.1.4 Characterisation: TEM images and the particle size distribution histogram were shown in Fig. 4*a*. It was observed that the prepared AuNPs were well dispersed, predominantly subspheroidal in shape with the size range from 8 to 25 nm (most of them were about 15 nm). HRTEM images (Fig. 4*b*) showed the clear lattice fringes of 0.23 nm, indicating the growth of the AuNPs occurred preferentially on the (111) plane [29]. This was further confirmed by XRD patterns. Insert fast Fourier transform (FFT) image also showed a crystalline pattern of the synthesised AuNPs.

The results of EDS analysis were shown in Fig. 5. A strong absorption peak was at 2.2 keV, which was a typical absorption peak of metallic Au [40]. The peaks at 8.4, 9.6 and 11.4 keV also showed the existence of elementary gold, which confirmed the composition of AuNPs.

The crystalline nature of the AgNPs was characterised by XRD. The XRD patterns were shown in Fig. 6. The diffraction peaks at (2θ) 38.30°, 44.28°, 64.62°, 77.57° and 81.75° were assigned to (111), (200), (220), (311) and (222) planes of the face-centered cubic (fcc) lattice of gold (JCPDS no. 04-0784) [41, 42]. The results demonstrated that the biosynthesised AuNPs were crystalline in nature. The size of AuNPs was calculated by Debye-Scherrer's equation was about 11 nm, which was in agreement with the result of TEM analysis.

3.1.5 FTIR analysis: FTIR analysis was performed to identify the functional groups in the peel and on the surface of AuNPs which were probably active for the reduction of chloroauric acid and the stabilisation of the synthesised AuNPs (Fig. 7). The FTIR spectra of both *C. maxima* peel and AuNPs were recorded. The FTIR spectra of *C. maxima* peel powder illustrated that the characteristic peaks appeared at 3413, 2927, 1619, 1056 and 622 cm^{-1}, respectively. The biosynthesised AuNPs also showed the

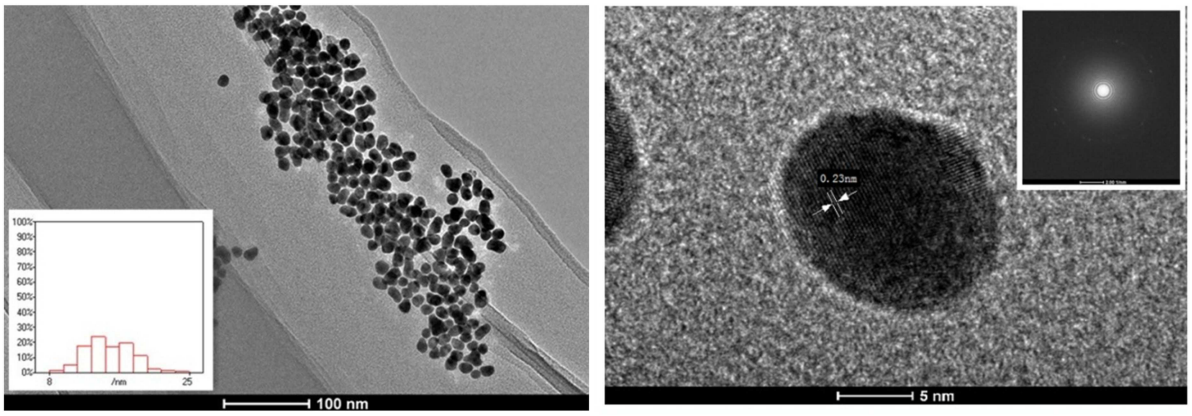

a *b*

Fig. 4 *TEM and HRTEM micrograph of synthesised AuNPs*
(a) TEM micrograph of synthesised AuNPs (inset shows size distribution histogram), and ***(b)*** HRTEM micrograph of synthesised AuNPs (inset correspond to FFT pattern)

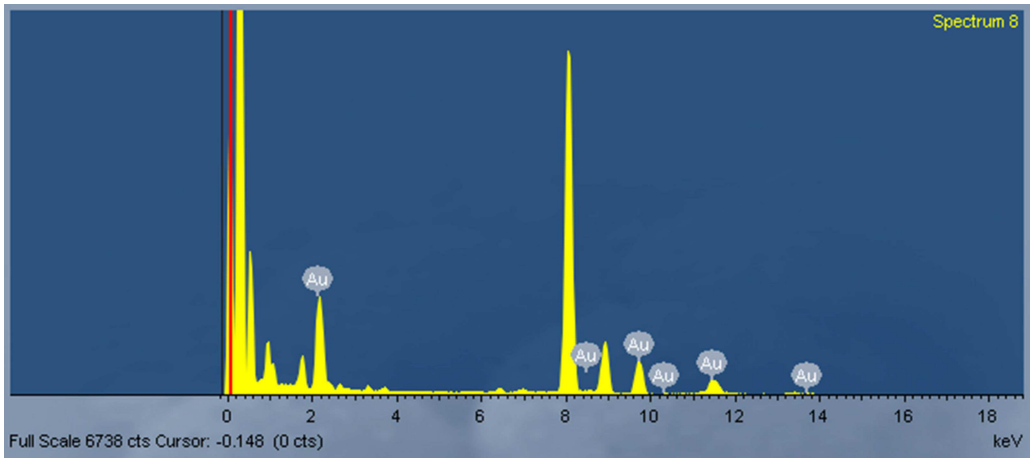

Fig. 5 *EDS analysis of synthesised AuNPs*

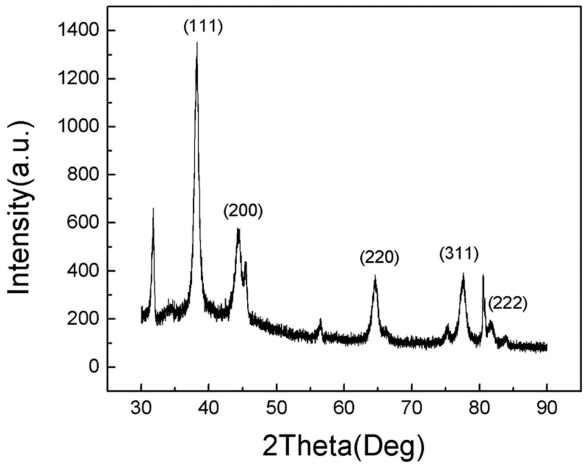

Fig. 6 *XRD pattern of the synthesised AuNPs*

characteristic peaks at 3411, 2925, 1619, 1051 and 622 cm^{-1}. The similar FTIR spectra demonstrated that the biosynthesised AuNPs were capped with the molecules from the peel. The peak at 1619 cm^{-1} was contributed to the stretching vibrations of C=C. The peak at around 3411 cm^{-1} corresponded to the stretching vibrations of O–H of phenols and carboxylic acids. The strong peak at 2925 cm^{-1} was assigned to the symmetric and asymmetric C–H stretching vibrations of aliphatic acids [43]. Other peaks at 1051 and 622 cm^{-1} might be assigned to ν(C–O) and δ(C–H) bending vibrations [44]. It has been confirmed naringin and hesperidin were the principal active components in the *C. maxima* peel [45]. Here, we speculated that flavonoids such like naringin and hesperdin probably acted as reducing agent and stabiliser that adhere on the surface of AuNPs to prevent agglomerating during the biosynthesis process [46].

3.2 Catalytic activity of AuNPs

It is well known that the bulk gold is chemically inert, but AuNPs exhibit excellent chemical activities and catalytic properties owing to the changing of redox potential from positive value to negative value [47]. Especially, the AuNPs with the small size can show the remarkable catalytic activity due to the increasing of the surface volume ratio and the enhancing of surface energy.

4-NP is a toxic water soluble compound which irritates the skin, eyes, and respiratory tract and inflammation [48]. Usually, 4-NP was converted to 4-AP to eliminate the toxicity of 4-NP. Herein, the catalytic activity of AuNPs was investigated by degrading 4-NP to 4-AP in the presence of $NaBH_4$. The process of degradation was monitored by UV–vis spectra. In the absence of $NaBH_4$, 4-NP showed a distinct peak at 320 nm. After addition of $NaBH_4$, the absorption peak shifted to ~400 nm because of the formation of 4-nitrophenolate ions [49]. Without any catalyst, the peak from 4-nitrophenolate ions remained unaltered for several days. However, when the biosynthesised AuNPs were added as catalysts, the intensity of the 4-nitrophenolate peak at 400 nm immediately decreased and a new peak at 310 nm appeared for the formation of 4-AP (Fig. 8*a*). Around 30 min, the colour of the mixture changed from yellow to colourless, and the peak at 400 nm disappeared, which indicated the degradation reaction completed.

The Langmuir and Hinshelwood model can be used to describe the relationship between the rate of the degradation of 4-NP in the presence of AuNPs with respect to time. Since the concentration of $NaBH_4$ was large enough compared with the concentration of 4-NP. Hence, the reaction rate (Ka) was only assumed to be dependent of the concentration of the 4-NP. The rate of equation

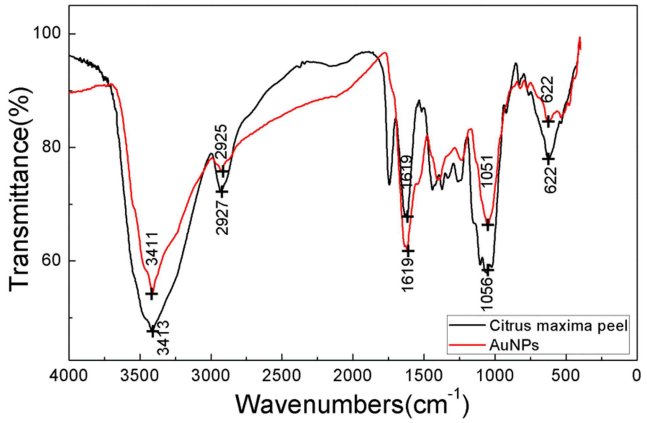

Fig. 7 *FTIR spectra of C. maxima peel and AuNPs*

can be simplified and integrated to be: $-Kat = \ln(C_t/C_0) = \ln(A_t/A_0)$; where C_t and A_t are the concentration and absorbance of reaction at any time, respectively, C_0 and A_0 are initial concentration and absorbance of reaction, respectively.

Plotting the $\ln(C_t/C_0)$ versus to the corresponding time (min) showed linear relationship in Fig. 8*b* and the rate constants were shown in Table 1. Obviously, the rate of degradation increased with the amount of AuNPs increasing. Therefore, the AuNPs synthesised using the extract of *C. maxima* peel showed a strong catalytic activity in the degradation of 4-NP, and it could be used for the treatment of organic wastewater.

Table 1 The rate constants for the degradation of 4-NP to 4-AP

Volume of Au nanoparticles solution, μL	Rate constant, min^{-1}
20	0.03164
40	0.06224
60	0.10999

3.3 Antibacterial activity

AuNPs have also attracted great attentions as a new class of biomedical materials, since they can act as both antibacterial and antifungal agents which are capable of interacting with microorganisms to produce cellular damage [50]. Fig. 9 shows the antibacterial activity of AuNPs which was tested against both gram negative (*E. coli*) and gram positive (*S. aureus*) bacteria. From the zones of inhibition, it was observed that *C. maxima* peel extract did not have any inhibitory effect on the bacterium growth, while the biosynthesised AuNPs exhibited a strong antibacterial effect. The inhibitory effect slightly increased with the concentration of AuNPs increasing according to the inhibition zones. Therefore, the biosynthesised AuNPs in our study have the potential to be used as effective disinfectants with good antibacterial activities.

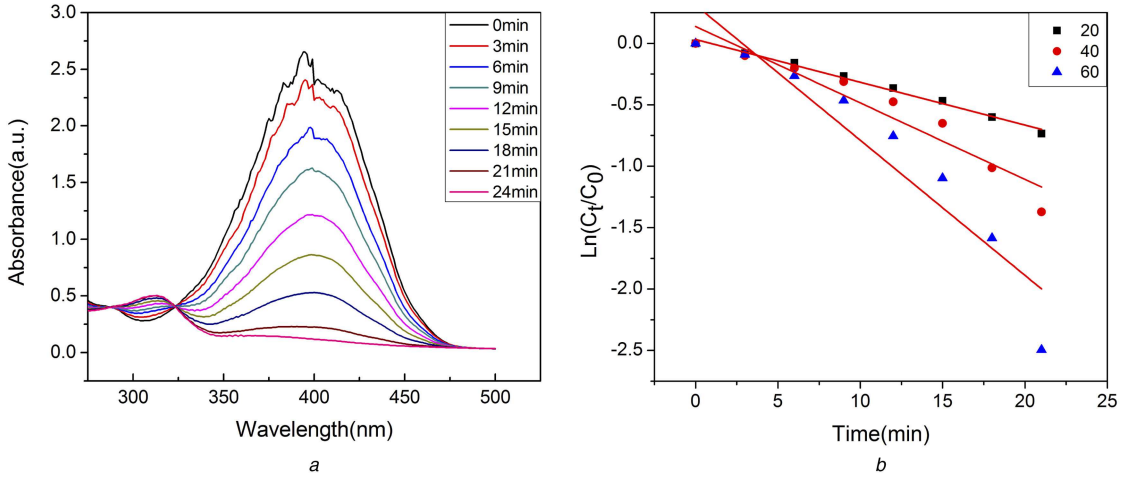

Fig. 8 *Biosynthesised AuNPs*
(a) UV–vis spectra of mixture of 4-NP and $NaBH_4$ in the presence AuNPs (60 μl), ***(b)*** Logarithm of the ratio between its final concentration and the initial concentration of 4-NP versus the corresponding time (min)

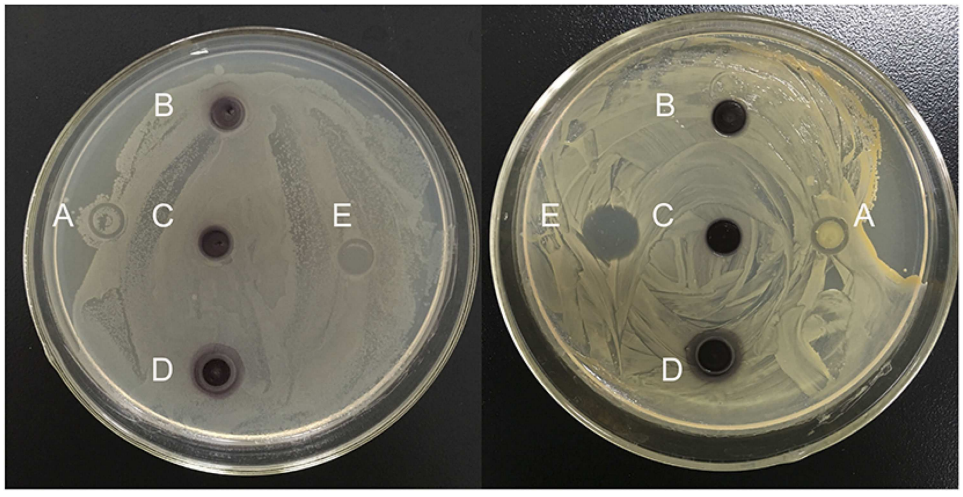

Fig. 9 *Antibacterial activities of the synthesised AuNPs against E. coli (A) and S. aureus (B)*
(a) *C. maxima* peel extract, ***(b)*** 1 mM AuNPs, ***(c)*** 1.5 mM AuNPs, ***(d)*** 2 mM AuNPs, ***(e)*** Gentamicin

4 Conclusion

One green method of biosynthesis of AuNPs was developed in our study. The extract of *C. maxima* peel was applied to synthesise AuNPs. The synthesis procedure was proved simple, cost effective and environment friendly. The morphologies of the AuNPs were characterised by TEM, EDS, XRD and FTIR, and the NPs were predominantly subspheroidal with the size range from 8 to 25 nm. The as-obtained AuNPs exhibited a strong catalytic activity in the degradation of 4-NP and an antibacterial activity against both *S. aureus* (gram positive) and *E. coli* (gram negative) bacteria.

5 Acknowledgments

This work was kindly co-funded by the National Natural Science Foundation of China (21277043, 21620102008), the Beijing Natural Science Foundation (8132038), and the Fundamental Research Funds for the Central Universities. The authors thank Ms. Weiping Cao in Plant Protection Institute, Hebei Academy of Agricultural and Forestry Sciences for her kindly help on their antibacterial experiments.

6 References

[1] Das, S.K., Das, A.R., Guha, A.K.: 'Gold nanoparticles: microbial synthesis and application in water hygiene management', *Langmuir*, 2009, **25**, (14), pp. 8192–8199

[2] Marie-Christine, D., Didier, A.: 'Gold nanoparticles: assembly, supramolecular chemistry, quantum-size-related properties, and applications toward biology, catalysis, and nanotechnology', *Chem. Rev.*, 2004, **104**, (1), pp. 293–346

[3] Jain, P.K., Lee, K.S., El-Sayed, I.H., *et al.*: 'Calculated absorption and scattering properties of gold nanoparticles of different size, shape, and composition: applications in biological imaging and biomedicine', *J. Phys. Chem. B*, 2006, **110**, (110), pp. 7238–7248

[4] Tang, H., Chen, J., Nie, L., *et al.*: 'A label-free electrochemical immunoassay for carcinoembryonic antigen (CAE) based on gold nanoparticles (AuNPs) and nonconductive polymer film', *Biosens. Bioelectron.*, 2007, **22**, (6), pp. 1061–1067

[5] Tong, L., Wei, Q., Wei, A., *et al.*: 'Gold nanorods as contrast agents for biological imaging: optical properties, surface conjugation and photothermal effects', *Photoch. Photobio.*, 2009, **85**, (1), pp. 21–32

[6] Boote, E., Fent, G., Kattumuri, V., *et al.*: 'Gold nanoparticle contrast in a phantom and juvenile swine: models for molecular imaging of human organs using X-ray computed tomography', *Acad. Radiol.*, 2010, **17**, (4), pp. 410–417

[7] Kunjiappan, S., Chowdhury, R., Bhattacharjee, C.: 'A green chemistry approach for the synthesis and characterization of bioactive gold nanoparticles using *Azolla Microphylla* methanol extract', *Front. Mater. Sci.*, 2014, **8**, (2), pp. 123–135

[8] Dong, C., Zhang, X., Cai, H.: 'Green synthesis of monodisperse silver nanoparticles using hydroxy propyl methyl cellulose', *J. Alloy Compd.*, 2014, **583**, (1), pp. 267–271

[9] Khatami, M., Pourseyedi, S.: '*Phoenix Dactylifera* (Date Palm) pit aqueous extract mediated novel route for synthesis high stable silver nanoparticles with high antifungal and antibacterial activity', *IET Nanobiotechnol.*, 2015, **9**, (4), pp. 184–190

[10] Kumar, B., Smita, K., Cumbal, L.: 'Biofabrication of nanogold from the flower extracts of *Lantana Camara*', *IET Nanobiotechnol.*, 2016, **10**, (3), pp. 154–157

[11] Mohanta, Y.K., Singdevsachan, S.K., Parida, U.K., *et al.*: 'Green synthesis and antimicrobial activity of silver nanoparticles using wild medicinal mushroom *Ganoderma Applanatum* (Pers.) Pat. from Similipal Biosphere Reserve, Odisha, India', *IET Nanobiotechnol.*, 2015, **9**, (6), pp. 184–189

[12] Soltani, N.M., Khatami, M., Shahidi Bonjar, G.H.: 'Extracellular synthesis gold nanotriangles using biomass of *Streptomyces microflavus*', *IET Nanobiotechnol.*, 2016, **10**, (1), pp. 33–38

[13] Nazeruddin, G.M., Prasad, N.R., Waghmare, S.R., *et al.*: 'Extracellular biosynthesis of silver nanoparticle using *Azadirachta Indica* leaf extract and its anti-microbial activity', *J. Alloy Compd.*, 2014, **583**, (583), pp. 272–277

[14] Sharma, J.K., Akhtar, M.S., Ameen, S., *et al.*: 'Green synthesis of CuO nanoparticles with leaf extract of *Calotropis Gigantea* and its dye-sensitized solar cells applications', *J. Alloy Compd.*, 2015, **632**, pp. 321–325

[15] Mohapatra, B., Kuriakose, S., Mohapatra, S.: 'Rapid green synthesis of silver nanoparticles and nanorods using *Piper Nigrum* extract', *J. Alloy Compd.*, 2015, **637**, (3), pp. 119–126

[16] Shankar, S.S., Ahmad, A., Pasricha, R., *et al.*: 'Bioreduction of chloroaurate ions by geranium leaves and its endophytic fungus yields gold nanoparticles of different shapes', *J. Mater. Chem.*, 2003, **13**, (7), pp. 1822–1826

[17] Shankar, S.S., Rai, A., Ahmad, A., *et al.*: 'Rapid synthesis of Au, Ag, and bimetallic Au core-Ag shell nanoparticles using Neem (*Azadirachta Indica*) leaf broth', *J. Colloid Interf. Sci.*, 2004, **275**, (2), pp. 496–502

[18] Shankar, S.S., Rai, A., Ankamwar, B., *et al.*: 'Biological synthesis of triangular gold nanoprisms', *Nat. Mater.*, 2004, **3**, (7), pp. 482–488

[19] Kumar, K.P., Paul, W., Sharma, C.P.: 'Green synthesis of gold nanoparticles with *Zingiber Officinale* extract: characterization and blood compatibility', *Process Biochem.*, 2011, **46**, (10), pp. 2007–2013

[20] Ghosh, S., Patil, S., Ahire, M., *et al.*: 'Synthesis of gold nanoanisotrops using *Dioscorea Bulbifera* tuber extract', *J. Nanomater.*, 2011, **2011**, (44), pp. 18083–18088

[21] Wang, Y., He, X., Wang, K., *et al.*: '*Barbated Skullcup* herb extract-mediated biosynthesis of gold nanoparticles and its primary application in electrochemistry', *Colloid Surf. B*, 2009, **73**, (1), pp. 75–79

[22] Thema, F.T., Beukes, P., Gurib-Fakim, A., *et al.*: 'Green synthesis of monteponite CdO nanoparticles by *Agathosma Betulina* natural extract', *J. Alloy Compd.*, 2015, **646**, pp. 1043–1048

[23] Diallo, A., Ngom, B.D., Park, E., *et al.*: 'Green synthesis of ZnO nanoparticles by *Aspalathus Linearis*: structural & optical properties', *J. Alloy Compd.*, 2015, **646**, pp. 425–430

[24] Sood, S., Arora, B., Bansal, S., *et al.*: 'Antioxidant, anti-inflammatory and analgesic potential of the *Citrus Decumana* L. peel extract', *Inflammopharmacology*, 2009, **17**, (5), pp. 267–274

[25] Xi, W., Fang, B., Zhao, Q., *et al.*: 'Flavonoid composition and antioxidant activities of Chinese local pummelo (*Citrus Grandis Osbeck*.) varieties', *Food Chem.*, 2014, **161**, (11), pp. 230–238

[26] Yu, J., Xu, D., Guan, H.N., *et al.*: 'Facile one-step green synthesis of gold nanoparticles using *Citrus maxima* aqueous extracts and its catalytic activity', *Mater. Lett.*, 2015, **166**, pp. 110–112

[27] Wei, Y., Fang, Z., Zheng, L., *et al.*: 'Green synthesis of Fe nanoparticles using *Citrus maxima* peels aqueous extracts', *Mater. Lett.*, 2016, **185**, pp. 384–386

[28] Zayed, M.F., Eisa, W.H.: '*Phoenix Dactylifera* L. leaf extract phytosynthesized gold nanoparticles; controlled synthesis and catalytic activity', *Spectrochim. Acta A*, 2013, **121C**, (1), pp. 238–244

[29] Paul, B., Bhuyan, B., Purkayastha, D.D., *et al.*: 'Green synthesis of gold nanoparticles using *Pogestemon Benghalensis* (B) O. Ktz. leaf extract and studies of their photocatalytic activity in degradation of methylene blue', *Mater. Lett.*, 2015, **148**, (12), pp. 37–40

[30] Das, S.K., Dickinson, C., Lafir, F., *et al.*: 'Synthesis, characterization and catalytic activity of gold nanoparticles biosynthesized with *Rhizopusoryzae* protein extract', *Green Chem.*, 2012, **14**, pp. 1322–1334

[31] Mubarakali, D., Thajuddin, N., Jeganathan, K., *et al.*: 'Plant extract mediated synthesis of silver and gold nanoparticles and its antibacterial activity against clinically isolated pathogens', *Colloid Surf. B*, 2011, **85**, (2), pp. 360–365

[32] Tamuly, C., Hazarika, M., Bordoloi, M.: 'Biosynthesis of Au nanoparticles by *Gymnocladus Assamicus* and its catalytic activity', *Mater. Lett.*, 2013, **108**, (5), pp. 276–279

[33] Amendola, V., Meneghetti, M.: 'Size evaluation of gold nanoparticles by UV−vis spectroscopy', *J. Phys. Chem. C*, 2009, **113**, (11), pp. 4277–4285

[34] Li, D., He, Q., Li, J.: 'Smart core/shell nanocomposites: intelligent polymers modified gold nanoparticles', *Adv. Colloid Interf. Sci.*, 2009, **149**, (1-2), pp. 28–38

[35] Srinath, B.S., Rai, R.V.: 'Biosynthesis of gold nanoparticles using extracellular molecules produced by *Enterobacter Aerogenes* and their catalytic study', *J. Clust. Sci.*, 2015, **26**, (5), pp. 1483–1494

[36] Basavegowda, N., Idhayadhulla, A., Yong, R.L.: 'Phyto-synthesis of gold nanoparticles using fruit extract of *Hovenia Dulcis* and their biological activities', *Ind. Crop. Prod.*, 2014, **52**, (52), pp. 745–751

[37] Shipway, A.N., Lahav, M., Rachel Gabai, A., *et al.*: 'Investigations into the electrostatically induced aggregation of Au nanoparticles', *Langmuir*, 2000, **16**, (23), pp. 8789–8795

[38] Link, S., El-Sayed, M.A.: 'Size and temperature dependence of the plasmon absorption of colloidal gold nanoparticles', *J. Phys. Chem. B*, 1999, **103**, (21), pp. 4212–4217

[39] Zhan, G., Huang, J., Lin, L., *et al.*: 'Synthesis of gold nanoparticles by *Cacumen Platycladi* leaf extract and its simulated solution: toward the plant-mediated biosynthetic mechanism', *J. Nanoparticle Res.*, 2011, **13**, (10), pp. 4957–4968

[40] Dauthal, P., Mukhopadhyay, M.: 'In-vitro free radical scavenging activity of biosynthesized gold and silver nanoparticles using *Prunus Armeniaca* (Apricot) fruit extract', *J. Nanoparticle Res.*, 2013, **15**, (1), pp. 1–11

[41] Emmanuel, R., Karuppiah, C., Chen, S.M., *et al.*: 'Green synthesis of gold nanoparticles for trace level detection of a hazardous pollutant (Nitrobenzene) causing methemoglobinaemia', *J. Hazard. Mater.*, 2014, **279**, pp. 117–124

[42] Muthuvel, A., Adavallan, K., Balamurugan, K., *et al.*: 'Biosynthesis of gold nanoparticles using *Solanum Nigrum* leaf extract and screening their free radical scavenging and antibacterial properties', *Biomed. Prevent. Nutr.*, 2014, **4**, (2), pp. 325–332

[43] Li, F.T., Yang, H., Zhao, Y., *et al.*: 'Novel modified pectin for heavy metal sdsorption', *Chin. Chem. Lett.*, 2007, **18**, (3), pp. 325–328

[44] Williams, D.H., Fleming, I.: '*Spectroscopic methods in organic chemistry*' (McGraw-Hill, 1980)

[45] Wu, T., Guan, Y., Ye, J.: 'Determination of flavonoids and ascorbic acid in grapefruit peel and juice by capillary electrophoresis with electrochemical detection', *Food Chem.*, 2007, **100**, (4), pp. 1573–1579

[46] Park, Y., Hong, Y.N., Weyers, A., *et al.*: 'Polysaccharides and phytochemicals: a natural reservoir for the green synthesis of gold and silver nanoparticles', *Chem. Inf.*, 2012, **5**, (6), pp. 69–78

[47] Hvolbæk, B., Janssens, T.V.W., Clausen, B.S., *et al.*: 'Catalytic activity of Au nanoparticles', *Nano Today*, 2007, **2**, (4), pp. 14–18

[48] Gu, S., Wunder, S., Lu, Y., *et al.*: 'Kinetic analysis of the catalytic reduction of 4-Nitrophenol by metallic nanoparticles', *J. Phys. Chem. C*, 2014, **118**, (32), pp. 18618–18625

[49] Muniyappan, N., Nagarajan, N.S.: 'Green synthesis of silver nanoparticles with *Dalbergia Spinosa* leaves and their applications in biological and catalytic activities', *Process Biochem.*, 2014, **49**, (6), pp. 1054–1061

[50] Hernández-Sierra, J.F., Ruiz, F., Pena, D.C.C., *et al.*: 'The antimicrobial sensitivity of streptococcus mutans to nanoparticles of silver, zinc oxide, and gold', *Nanomed. Nanotechnol. Biol. Med.*, 2008, **4**, (3), pp. 237–240